

Differential involvement of corticospinal tract (CST) fibers in UMN-predominant ALS patients with or without CST hyperintensity: A diffusion tensor tractography study



Venkateswaran Rajagopalan^{a,b}, Erik P. Pioro^{c,d,*}

^aDepartment of Electrical and Electronics Engineering, Birla Institute of Technology and Science Pilani, Hyderabad Campus, Hyderabad, 500078, India

^bDepartment of Biomedical Engineering, Lerner Research Institute, Cleveland Clinic, Cleveland, OH 44195, United States

^cNeuromuscular Center, Department of Neurology, Neurological Institute, Cleveland Clinic, Cleveland, OH 44195, United States

^dDepartment of Neurosciences, Lerner Research Institute, Cleveland Clinic, Cleveland, OH 44195, United States

ARTICLE INFO

Article history:

Received 10 November 2016

Received in revised form 20 February 2017

Accepted 21 February 2017

Available online 22 February 2017

Keywords:

DTI

ALS

Phenotypes

Diffusion tensor tractography

ABSTRACT

Diagnosis of amyotrophic lateral sclerosis (ALS) depends on clinical evidence of combined upper motor neuron (UMN) and lower motor neuron (LMN) degeneration, although ALS patients can present with features predominantly of one or the other. Some UMN-predominant patients show hyperintense signal along the intracranial corticospinal tract (CST) on T2- and proton density (PD)-weighted images (ALS-CST+), and appear to have faster disease progression when compared to those without CST hyperintensity (ALS-CST-). The reason for this is unknown. We hypothesized that diffusion tensor tractography (DTT) would reveal differences in DTI abnormalities along the intracranial CST between these two patient subgroups. Clinical DTI scans were obtained at 1.5T in 14 neurologic controls and 45 ALS patients categorized into two UMN phenotypes based on clinical measures and MRI. DTT was used to quantitatively assess the CST in control and ALS groups.

DTT revealed subcortical loss ('truncation') of virtual motor CST fibers (presumably) projecting from the precentral gyrus (PrG) in ALS patients but not in controls; in contrast, virtual fibers (presumably) projecting to the adjacent postcentral gyrus (PoG) were spared. No significant differences in virtual CST fiber length were observed between controls and ALS patients. However, the frequency of CST truncation was significantly higher in the ALS-CST+ subgroup (9 of 21) than in the ALS-CST- subgroup (4 of 24; $p = 0.049$), suggesting this finding could differentiate these ALS subgroups. Also, because virtual CST truncation occurred only in the ALS patient group and not in the control group ($p = 0.018$), this DTT finding could prove to be a diagnostic biomarker of ALS. Significantly shorter disease duration and faster disease progression rate were observed in ALS patients with CST fiber truncation than in those without ($p < 0.05$). DTI metrics of fractional anisotropy (FA), mean diffusivity (MD), axial diffusivity (AD) and radial diffusivity (RD) were also determined in four regions of interest (ROIs) along the CST, namely: cerebral peduncle (CP), posterior limb of internal capsule (PLIC), centrum semiovale at top of lateral ventricle (CSoLV) and subcortical to primary motor cortex (subPMC). Of note, FA values along the left hemisphere virtual CST tract were significantly different between controls and ALS-CST+ patients ($p < 0.05$) only at the PLIC level, but not at the CSoLV or subPMC level. Also, no significant differences in FA values were observed between ALS subgroups or between control and ALS-CST- groups ($p > 0.05$) in any of the ROIs. In addition, comparing FA values between ALS patients with CST truncation and those without in the aforementioned four ROIs, revealed no significant differences in either hemisphere. However, visual evaluation of DTT was able to identify UMN degeneration in patients with ALS, particularly in those with a more aggressive clinical disease course and possibly different pathologic processes.

© 2017 The Authors. Published by Elsevier Inc. This is an open access article under the CC BY-NC-ND license (<http://creativecommons.org/licenses/by-nc-nd/4.0/>).

Abbreviations: ALS, Amyotrophic lateral sclerosis; cMRI, Conventional MRI; CNS, Central nervous system; CP, Cerebral peduncle; CSoLV, Centrum semiovale at top of lateral ventricle; CST, Corticospinal tract; DTI, Diffusion tensor imaging; DTT, Diffusion tensor tractography; DW, Diffusion weighted; EMG, Electromyography; EPI, Echo planar imaging; FA, Fractional anisotropy; FLAIR, Fluid attenuated inversion recovery; FSE, Fast spin echo; LMN, Lower motor neuron; MD, Mean diffusivity; MR, Magnetic resonance; MRI, Magnetic resonance imaging; PD, Proton density; PLIC, Posterior limb of the internal capsule; PMC, Primary motor cortex; PoG, Postcentral gyrus; PrG, Precentral gyrus; PSC, Primary sensory cortex; ROI, Region of interest; SNR, Signal-to-noise ratio; SS-EPI, Single shot echo planar imaging; SubPMC, Subcortical to primary motor cortex; TE, Echo time; TR, Repetition time; UMN, Upper motor neuron.

* Corresponding author at: Neuromuscular Center, S90, Cleveland Clinic, 9500 Euclid Avenue, Cleveland, OH 44195, United States.

E-mail address: PIOROE@ccf.org (E.P. Pioro).

1. Introduction

Amyotrophic lateral sclerosis (ALS) is a progressive motor neuron disorder with no known cure. Current delay to diagnosis is approximately 12 months from onset of symptoms and only 60% of cases are diagnosed correctly on their initial evaluation (Mitusmoto et al., 1998). Current ALS diagnosis is based on clinical signs and symptoms and by excluding conditions that mimic ALS (Mitusmoto et al., 1998). According to the revised El Escorial criteria (Brooks et al., 2000), ALS diagnosis is based on the presence of both upper motor neuron (UMN) and lower motor neuron (LMN) signs which cannot be explained by other causes. One of the main pathologic hallmarks of ALS is the UMN degeneration of corticospinal tract (CST) from precentral gyrus (PrG) passing through internal capsule to spinal cord (da Rocha et al., 2004). Electromyography (EMG) is an objective test for LMN degeneration, but no easily accessible equivalent test exists to objectively identify UMN dysfunction (Mitusmoto et al., 1998). This can contribute to delays in clinical diagnosis of ALS (Kaufmann et al., 2004). Therefore, there is interest in identifying biomarkers of UMN degeneration in ALS to allow early diagnosis, recognize disease subtypes (which exist phenotypically), monitor disease progression and assess the efficacy of therapeutic interventions.

Even though ALS patients have clinical evidence of both UMN and LMN dysfunction, a proportion of patients begin with UMN abnormalities before developing identifiable LMN signs. Earlier studies have observed that between 17% and 67% (median 40%) of ALS patients with predominant UMN signs have bilateral CST hyperintensity visible on conventional T2-, proton density (PD)-, and fluid attenuated inversion recovery (FLAIR)-weighted images (Mitusmoto et al., 1998). While we too have found a proportion of UMN-predominant ALS patients to have CST hyperintensity, other patients with similar clinical features do not. Of note, UMN-predominant ALS patients with CST hyperintensity are significantly younger (Mitusmoto et al., 1998; Matte and Pioro, 2010), have faster disease progression rate (Matte and Pioro, 2010) and shorter survival period (Matte and Pioro, 2010) compared to those without CST hyperintensity. The reason for this discrepancy is unclear and the underlying pathologic substrate causing these changes is unknown.

Most previous MRI brain studies in ALS have identified such CST hyperintensity qualitatively (i.e. relying on visual evaluation) using conventional MRI (cMRI) such as T2-, PD-, and FLAIR-weighted images (Mitusmoto et al., 1998; da Rocha et al., 2004; Ngai et al., 2007), which is prone to error and does not provide quantitative evidence of underlying neuronal changes causing the signal change. Diffusion tensor imaging (DTI) quantifies the directional movement of water molecules at the microscopic level, which is not feasible with cMRI. Therefore, DTI has been used to non-invasively evaluate pathophysiological changes in the CNS of patients with various neurodegenerative diseases, including ALS (Ellis et al., 1999). An elegant feature of DTI is its ability to reconstruct virtual neural fiber tracts (“tractography”), which is not possible with cMRI techniques.

We objectively identified virtual CST fibers with diffusion tensor tractography (DTT) to determine non-invasively and visually if ALS patients could be distinguished from neurologic controls as well as from each other, depending on the presence or absence of CST hyperintensity identified by cMRI. We hypothesized that the qualitative presence or absence of CST hyperintensity on cMRI would be objectively identified by DTT in the form of truncated virtual motor fibers. Truncation of virtual hyperintense but not non-hyperintense CST fibers would support the presence of different underlying pathological substrates in such UMN-predominant ALS patients and potentially represent differing disease mechanisms.

2. Method

2.1. Patient demographics

2.1.1. Data acquisition

DTI data obtained as part of clinical neuroimaging evaluation were approved by the Institutional Review Board at Cleveland Clinic to be

stored and analyzed as de-identified images after patients provided verbal consent. DTI data were obtained in 14 neurological controls (with non ALS-mimic diagnoses indicated in Supplementary Table 1) and in 45 ALS patients with the following clinical phenotypes: UMN-predominant with CST hyperintensity (ALS-CST+) ($n = 21$, 14 male, 7 female, aged 52.3 ± 11.4 , mean \pm SD), and UMN-predominant without CST hyperintensity (ALS-CST-) ($n = 24$, 13 male, 11 female, aged 58.3 ± 11.4). UMN-predominant ALS patients were those in whom LMN signs were either undetectable, or restricted to only one neuraxial level (bulbar, cervical, or lumbosacral) at the time of MRI. UMN patients with CST hyperintensity were those in whom hyperintense signal was observed along the CST in both T2- and PD-weighted images. Clinical features of ALS patients are given in Table 1.

2.2. Imaging protocol

2.2.1. Diffusion tensor imaging protocol

DTI data were acquired on a 1.5T magnet (Siemens Symphony, Erlangen, Germany) using single shot-echo planar imaging (SS-EPI) sequence along 12 diffusion weighted ($b = 1000 \text{ s/mm}^2$) directions and one $b = 0 \text{ s/mm}^2$. Imaging parameters were: 30 slices, 4-mm thick, with $1.9 \times 1.9 \text{ mm}$ in-plane resolution; pulse sequence parameters were: repetition time TR = 6000 ms, echo time TE = 121 ms, EPI factor = 128, and scan time = 7.54 min.

2.2.2. Field map imaging protocol

Gradient-echo field maps were acquired to correct for geometrical distortion caused by susceptibility artifacts. Field map imaging parameters were: number of slices = 30, slice thickness = 4 mm, slice gap = 4 mm, TR = 500 ms, TEs = 6.11 ms and 10.87 ms.

2.2.3. T2- and PD-weighted imaging protocol

CST hyperintensity was assessed using T2- and PD-weighted images obtained using dual-echo fast spin echo (FSE) sequence whose imaging parameters were: 40 contiguous slices, slice thickness = 4 mm, in-plane resolution = $0.9 \times 0.9 \text{ mm}$; TR = 3900 ms, TEs = 26 ms and 104 ms, total scan time = 3.5 min.

2.3. Data processing

DTI images were first corrected for susceptibility artifacts using FSL's FUGUE (Jenkinson, 2003; Jenkinson, 2004; Smith et al., 2004) and then for eddy current distortion effects. The b-matrix was rotated in order to preserve correct orientation information (Leemans and Jones, 2009; Sage et al., 2009). These images were then processed using DTI Studio open software (https://www.nitrc.org/projects/mri_studio/) and DTT of CST was performed in the following manner (Jiang et al., 2006). Virtual neural fibers were reconstructed using the fiber assignment by

Table 1
Clinical parameters of ALS patients.

Clinical measure/ALS subgroups	ALS-CST+ mean \pm SD	ALS-CST- mean \pm SD	<i>p</i>
<i>n</i>	21	24	NS
Age (years)	52.3 \pm 11.4	59.5 \pm 12.1	<0.05
Symptom duration prior to MRI (months)	9.6 \pm 5.5	36.4 \pm 44.2	<0.001
ALSFRR-R score	34.6 \pm 7.8	34.1 \pm 8.1	NS
Disease progression rate	1.38 \pm 1.64	0.46 \pm 0.43	0.001

Key:

SD - Standard deviation.

ALS-CST+ - ALS patients with predominant upper motor neuron (UMN) signs and hyperintense signal along the corticospinal tract (CST) on conventional proton density (PD) and T2-weighted images and no clinical dementia.

ALS-CST- - ALS patients with predominant UMN signs without CST hyperintensity and no clinical dementia (ALS-CST-).

ALSFRR-R - ALS functional rating score-revised.

NS - Not significant.

continuous tracking (FACT) algorithm described in detail elsewhere (Jiang et al., 2006). Fiber tracking parameters were initiated from every voxel (Wakana et al., 2007) with FA = 0, threshold for termination at 0.2, and track turning angle of 41°. After the above preliminary processing steps, CST fiber tracts on both sides were reconstructed after Wakana et al. (Wakana et al., 2007) by placing a region of interest (ROI) first caudally in the cerebral peduncle and second rostrally just beneath the primary motor cortex (PMC), as previously described (Rajagopalan et al., 2013).

2.4. DTT and clinical measures

For the purposes of this tractography study, virtual CST fibers are ‘truncated’ when they are absent in the immediate subcortical white matter region of one or both hemispheres, extending only between the upper level of the lateral ventricles and brainstem (tracts in red shown in Fig. 1b). We quantified truncation by measuring average virtual CST fiber length (in each of left and right hemispheres) in ALS patient groups and controls. Average CST fiber length represents the mean length of all fibers in the entire CST bundle, as reconstructed in each subject; please refer to the manual of DTI studio software for more details. To measure average CST fiber length in ALS patients, we grouped them by presence or absence of virtual tract truncation, thereby pooling ALS-CST+ and ALS-CST– patient subgroups. SPSS 16.0 was used for statistical comparisons of measures between control and patient groups, and among ALS subgroups. Frequency of CST truncation between ALS-CST+ and ALS-CST– subgroups was tested using Fisher's Exact Test. One-way ANOVA was used to compare CST fiber length between control, ALS-CST+ and ALS-CST– groups. Student's *t*-test was used to compare average CST fiber length between ALS patients showing truncation and no truncation.

We measured fractional anisotropy (FA) along virtual CST fibers in ALS-CST+ and ALS-CST– patients using the ROI approach to compare with DTT-derived findings. Susumu Mori and colleagues (Wakana et al., 2004) created a CST fiber tract probability atlas template using DTI data of healthy controls. Because this CST atlas is in MNI space, we registered all our subjects' data to this atlas using FSL's linear and non-linear registration tools. The CST atlas was brought to subject's space to identify ROIs at four levels along the CST, namely, cerebral peduncle (CP), posterior limb of the internal capsule (PLIC), centrum semiovale at top of lateral ventricle (CSoLV), and subcortical to primary motor cortex (subPMC) in each of the controls and ALS patients. After FA values were measured in each of these ROIs, one-way ANOVA was used to compare them between control and ALS patient groups. Disease duration, ALSFRS-R score, and disease progression rate were compared between ALS subgroups and also between patients with CST truncation and those without truncation using appropriate statistical models. Clinical and DTT measures were correlated using Spearman's correlation.

3. Results

3.1. Tractography

When reconstructing virtual subPMC CST fibers by tractography, we observed their absence (truncation) between the CSoLV level and PrG (or primary motor cortex, PMC) in some patients from both UMN-predominant ALS subgroups. Truncation was detected primarily in the ALS-CST+ subgroup (9 of 21, 42.8%;) and less frequently in the ALS-CST– subgroup (4 of 24, 16.6%; $p = 0.049$). Of note, CST was not truncated in any control subjects. The frequency of CST truncation in the ALS group as a whole (both ALS-CST+ and ALS-CST– combined) was significantly ($p = 0.018$) higher than in the control group. Fig. 1 shows virtual CST fibers extending between motor cortex and subcortical white matter in a typical control subject but not in an ALS patient because of truncation. Compared with ALS patients showing no CST truncation, those with truncation tended to be younger ($p = 0.05$), had significantly shorter disease duration ($p = 0.001$) and a faster rate of disease progression ($p = 0.001$) (Table 1).

One-way ANOVA showed no significant differences in virtual CST fiber length between controls and ALS patients ($F = 1.064$, $p = 0.352$). Of note, average CST length in the right hemisphere was significantly shorter in the ALS CST truncated group (mean = 60.7 mm) compared to ALS patients without truncation (mean = 76.3 mm, $p = 0.001$). In the left hemisphere, however, no significant difference in CST length was observed between ALS patients with or without CST truncation. Table 2 gives average virtual CST fiber length for controls and ALS patients.

We also investigated whether truncation of virtual tracts affected nonmotor tracts connecting the PoG (or primary sensory cortex, PSC) with subcortical white matter. Most of these fibers should be afferents to the cortex and therefore relatively spared from cortical motor neuron degeneration. After reconstructing these tracts by placing the second ROI over the PSC, we found they were much less frequently truncated than motor CST fibers (Fig. 2). In fact, truncation of such virtual tracts occurred in only 1 subject from each of the ALS patient subgroups, i.e. 1 of 21 (4.7%) in ALS-CST+, and 1 of 24 (4.1%) in ALS-CST– subgroups. Because scans from all subject groups were obtained and processed in the same way, methodological differences would not be expected to explain these findings. We systematically investigated potential influence of image acquisition and processing techniques on CST truncation, and provide details in the Supplementary Material.

The ROI approach to analysis (using CST atlas) showed that FA values along the left hemisphere virtual CST tract were significantly different ($p < 0.05$) between controls and ALS-CST+ patients only at PLIC level, but not at CSoLV or subPMC levels. Also, no significant ($p > 0.05$) differences in FA values were observed between ALS subgroups or between control and ALS-CST– groups in any of the ROIs. In addition,

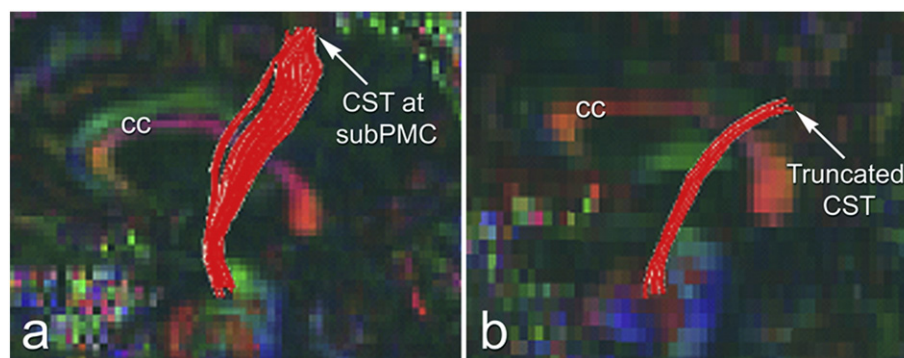


Fig. 1. FA color maps (sagittal views) show tractography-derived CST fibers extending subcortically from subjacent to the primary motor cortex (subPMC), which are intact in a control subject (a), and truncated in a patient with UMN-predominant ALS (b). cc, corpus callosum.

Table 2
Average virtual CST fiber length.

Subjects (sample size, <i>n</i>)	Left CST length (mm) mean ± SD	Right CST length (mm) mean ± SD
Controls (<i>n</i> = 14)	72.19 ± 8.07	72.92 ± 4.97
ALS-CST+ (<i>n</i> = 21)	74.47 ± 12.04	71.57 ± 13.31
ALS-CST- (<i>n</i> = 24)	76.29 ± 8.32	74.51 ± 8.34
ALS patients with CST truncation (<i>n</i> = 13)	75.32 ± 11.39	60.69 ± 13.02*
ALS patients without CST truncation (<i>n</i> = 32)	74.88 ± 9.73	76.25 ± 5.48

Key:

SD - Standard deviation.

n - sample size.

NS - Not significant.

* *p* = 0.001.

we also compared FA values between ALS patients with CST truncation and those without in all the four ROIs mentioned above. Student's *t*-test found no significant differences in FA values of any ROIs in either left or right hemisphere CST between these patient subgroups.

3.2. Clinical measures

No significant (*p* > 0.05) correlations were observed between CST fiber length (right and left hemisphere virtual fibers analyzed separately), and symptom duration, disease progression rate, or ALSFRS-R score in both CST-truncated and -nontruncated ALS subgroups. Symptom duration was significantly (*p* < 0.001) shorter in the ALS-CST+ subgroup than in the ALS-CST- subgroup. Of note, patients in the ALS-CST+ subgroup had significantly (*p* = 0.001) faster disease progression than those in ALS-CST- subgroup at the time of MRI. Also, the ALS-CST+ subgroup tended to be younger (*p* = 0.05) when compared to the ALS-CST- subgroup.

4. Discussion

This study demonstrates that virtual fibers in the subcortical white matter appear disrupted ('truncated'): (1) in the descending CST of patients with ALS compared to neurologic controls; (2) if connecting with the PrG (or PMC), and not with PoG (or PSC), the former presumably representing descending motor CST fibers and the latter representing ascending sensory afferents; (3) significantly more frequently in the CST of UMN-predominant ALS patients with CST hyperintensity (42.8%) compared to those without (16.6%); (4) in ALS patients with significantly faster disease progression rate and shorter disease duration.

Descending motor pathways in the CST are primarily implicated in ALS while ascending sensory pathways are not. Presently, no quantitative biomarker is available to assess UMN CST changes. We show here for the first time that DTT detects virtual motor CST fiber disruption in UMN-predominant ALS patients compared to controls, while nearby

presumably ascending sensory tracts are spared. CST truncation does not occur in any of the control subjects studied at 1.5T (*n* = 12) and at 3T (*n* = 14) (see Supplementary Material for details). Our DTT findings of virtual motor fiber disruption between only PrG and centrum semiovale in these UMN-predominant ALS patients indicate that CST fibers are more often affected rostrally than caudally, i.e. closer to the motor neuron cell body. This is in contrast to more distal fibers at the PLIC level showing diminished FA values in the left hemisphere of ALS patients with CST truncation.

Previous studies in ALS reported reduction in FA values especially in the PLIC level in ALS compared to controls (Ellis et al., 1999; Abe et al., 2004; Graham et al., 2004; Jacob et al., 2003; Sach et al., 2004; Schimrigk et al., 2007) using ROI identification. None of these studies reported CST fiber loss in ALS, which may be due to the limitation of the ROI approach. Furthermore, ROI identification used in previous studies (Graham et al., 2004; Jacob et al., 2003; Sach et al., 2004; Schimrigk et al., 2007) was limited to certain CST levels and DTI metrics were mainly used. We did not observe any significant differences in FA values between controls and ALS patients and among the ALS subgroups in CSoLV and subPMC using the ROI approach. In addition, we did not observe any significant differences in FA values in any of the four ROIs along CST virtual fiber tracts between ALS patients with and without CST truncation. In contrast, DTT revealed significant differences of CST truncation and CST fiber length between ALS patients with and without CST truncation. Our results suggest that DTT is more likely to detect CST damage anywhere along its entire length compared to DTI metrics of specific levels using an ROI approach.

Our DTT finding of subcortical fiber truncation in patients arising from the PMC and not those connecting with the PSC suggests specificity of this finding to motor pathways. Whatever pathophysiologic process causes truncation, it appears to be fiber-type specific. This is in keeping with relative sparing of the sensory system in ALS with <15% of ALS patients reporting sensory symptoms (Gubbay et al., 1985; Medina and Gavia, 2008). In fact, only one individual from each ALS subgroup displayed truncation along virtual sensory tracts connecting with the PSC. In addition to the above-mentioned DTT differences between CST (motor) and non-CST (sensory) fibers, significant differences existed in CST virtual fiber integrity between ALS-CST+ and ALS-CST- subgroups. A prominent CST truncation effect (42.8%) was observed in ALS-CST+ patients compared to ALS-CST- (16.6%) patients. This observation provides further imaging evidence of a structural difference between these subgroups, which may result from divergent pathologies affecting CST fibers. DTT differences between ALS-CST+ and ALS-CST- subgroups are supplemented by observed clinical findings of significantly shorter symptom duration and faster disease progression rate in the former compared to latter patient subgroups. Importantly, the differential involvement of motor but not sensory fibers, truncation occurring more frequently in one ALS phenotype than others and no truncation in controls all suggest that virtual CST interruption/truncation is specific to fiber- and disease-type. It is unclear why patients in the ALS-CST+ subgroup have significantly shorter disease duration and

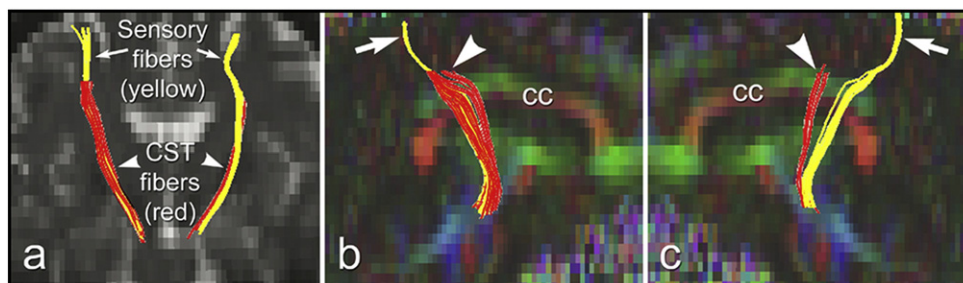


Fig. 2. Truncation of virtual CST fibers arising from primary motor cortex (red, arrowheads) compared with fibers projecting to/from sensory cortex (yellow, arrows) in an UMN-predominant ALS patient with faster disease progression rate. Tracts are shown projected on a coronal b0 image (a), and on sagittal images in right hemisphere (b), and left hemisphere (c). cc, corpus callosum.

faster disease progression rate when compared to ALS-CST – patient subgroup. Furthermore, ALS patients with CST hyperintensity have shorter survival period on average (3.5 years) compared to those with hypointensity of the primary motor cortex (7 years) (Matte and Pioro, 2010). Does the occurrence of CST hyperintensity with faster disease progression and shorter disease duration in the ALS-CST + patient subgroup correspond to different pathophysiological mechanisms of disease from those in the ALS-CST – patient subgroup? Our findings show that truncation of virtual motor CST fibers correlates significantly with disease duration and progression rate. Although this suggests the underlying process causing CST fiber truncation is associated with faster disease progression in such patients, a causative role cannot be implied.

Many neuroimaging studies that evaluated CST hyperintensities in UMN-predominant ALS patients using T2-, PD- and FLAIR-weighted MRI (da Rocha et al., 2004; Ngai et al., 2007) showed inconsistent findings probably due to their qualitative nature and study of varied and individual CST levels (e.g. subjacent to precentral gyrus, in centrum semiovale, etc.). They speculated that the hyperintense signal along the CST was due to the cellular changes of neuronal degeneration. One radiologic-pathologic study reporting CST degeneration examined only the posterior limb of the internal capsule (Yagishita et al., 1994). No quantitative evidence exists of CST disruption and damage in patients with such hyperintense signals. Also, it is unknown why certain ALS patients with predominant UMN signs have CST hyperintensity while others do not. Although our DTT results do not answer that question directly, they do provide evidence of CST fiber disruption occurring primarily in ALS patients with CST + hyperintensity, and localize at least one component of this pathologic change to the rostral CST. Importantly, whatever process causes virtual CST truncation detected by DTT, it is certainly not the result of actual axonal loss (wallerian degeneration). This would result in loss of virtual fibers *distal*, not proximal, to the truncated segment because relative to the neuronal cell body, axonal lesions cause degeneration of distal (not proximal) segments. Therefore, our findings suggest microanatomic pathology extrinsic to CST fibers, as could result from focal astrogliosis or microgliosis, disrupting creation of virtual tracts. It is unlikely that the superior longitudinal fasciculus traversing perpendicular to descending CST at this level causes virtual fiber truncation because all patient (and probably control) groups and presumed ascending sensory tracts should be affected similarly.

We found the average CST bundle length to be significantly shorter in the right hemisphere of ALS patients with CST truncation compared to those without. This concurs with our observation that CST truncation in 17 of 18 ALS patients (from both ALS-CST + and ALS-CST – groups) occurred in the right hemisphere, and in only 4 of 18 patients in the left hemisphere. We suspect this small sample size prevented detecting a significant difference in average CST bundle length in the left hemisphere of ALS patients with CST truncation compared to those without.

In our experience, we found DTT to be the preferred approach to study DTI metrics over manually tracing the ROI because DTT: (1) provides more accurate identification of the CST; (2) is highly reproducible; (3) is less time intensive. In addition, DTT can delineate different neural fiber types, which an ROI approach cannot do. For example, DTT could differentiate descending motor CST fibers (presumably arising from the PrG) from ascending sensory fibers (presumably projecting to the PoG), whereas an ROI approach could not because motor and sensory fibers intermingle in subcortical regions. Nonetheless, CST truncation in ALS patients indirectly reflects a reduction of FA values by revealing decreased virtual nerve fiber integrity. Specifically, the tractography algorithm is based on FA values which dictate the starting and stopping of fiber tracking; we assigned FA = 0.2 threshold to stop fiber tracking and avoid reconstructing tracts in grey matter regions (FA for grey matter is <0.2). Therefore, absence of virtual tract formation (i.e., truncation) in these CST regions indicates FA < 0.2, which in white matter of ALS patients represents reduced virtual fiber tract integrity.

We examined whether CST truncation could have been artefactual because of poor quality DTI data, i.e., low signal-to-noise ratio (SNR),

low resolution, anisotropic voxels, or from the tractography reconstruction algorithm used. These factors were evaluated using a 3T MRI DTI dataset of different ALS patients, whose images had utilized isotropic voxel dimensions and higher SNR (see Supplementary Material for details). Similar to our 1.5T findings, CST truncation was observed in only ALS patients and not in controls scanned at 3T. Therefore, the consistent observation of CST truncation only in ALS patients and not in controls at both magnet strengths indicates that scan quality at 1.5T, including resolution, anisotropic voxel dimension and SNR does not appear to cause CST truncation. To assess whether the deterministic tracking algorithm used here contributed to truncation, we re-analyzed the data with a probabilistic tractography algorithm that takes into account the uncertainty of tensor model fit and can extend through lesions. However, CST truncation persisted in the same patients even when probabilistic tracking was used, demonstrating its independence from the fiber-tracking algorithm used. Therefore, these tests demonstrated that acquisition protocols and image processing algorithms did not lead to CST truncation.

In summary, the correlation of virtual CST fiber truncation with shorter disease duration and faster disease progression rate in some ALS patients suggests that DTT can be used to distinguish between patient subgroups and possibly identify a more severe pathologic process. In addition, CST truncation occurring only in ALS patients and not in controls suggests that this DTT finding may prove to be a diagnostic biomarker of ALS. Not only does identifying these MRI changes at 1.5T and utilizing only 12 directions indicate their robustness, detecting them using relatively routine clinical MRI protocols provides an easily accessible technique. Differences in DTT between ALS-CST + and ALS-CST – subgroups are supplemented by the observed clinical findings of significantly shorter duration of symptoms and faster disease progression in the former compared to latter patient subgroups. Together, these observations suggest unique pathologies along the CST in these two patient subgroups. Persistence of virtual CST truncation at 1.5T and 3T in only ALS patients suggests it reflects a real difference in extra-axonal microanatomic pathology near the subcortical level of these fibers. Future studies correlating our DTT findings with histopathology are necessary to explore this possibility.

5. Conclusion

Using brain images from patients with ALS obtained during routine clinical MRI at 1.5T, we have found differences in DTT/DTI metrics between subgroups identified by clinical phenotypes. Importantly, we found ALS-CST + patients with rapidly progressing disease to more frequently show rostral truncation of virtual CST fibers generated by tractography, compared to ALS-CST – patients with slower disease progression. Our DTT finding in only ALS patients of truncated subcortical fibers arising from the PMC but not those connecting with PSC suggests fiber-type specificity, and aligns with the relative sparing of the sensory system in ALS. Right hemisphere CST fiber bundle was significantly shorter in the ALS CST truncated group when compared to ALS patients without CST truncation. Correlation of virtual CST fiber truncation with shorter disease duration and faster progression in ALS-CST + patients suggests that DTT can identify a more severe pathologic condition in some ALS patients and distinguish between patient subgroups. The identification of the microanatomic change(s) resulting in this truncation remain(s) to be identified and may provide clues to underlying pathogenic processes.

Author contributions

Venkateswaran Rajagopalan - acquired and processed data, analyzed the results, and wrote the manuscript.

Erik P. Pioro - designed the study, acquired data, analyzed the results, and made extensive revisions on the manuscript.

Conflict of interest

The authors do not have any conflict of interest to disclose.

Acknowledgement

The authors thank all the patients who participated in this study and Dr. Guang H Yue for providing facilities to process the data as well as his comments to improve the manuscript.

References

- Abe, O., Yamada, H., Masutani, Y., Aoki, S., Kunimatsu, A., Yamasue, H., et al., 2004 Oct. Amyotrophic lateral sclerosis: diffusion tensor tractography and voxel-based analysis. *NMR Biomed.* 17 (6):411–416 (PubMed PMID: 15386625). Epub 2004/09/24. eng).
- Brooks, B.R., Miller, R.G., Swash, M., Munsat, T.L., 2000 Dec. El Escorial revisited: revised criteria for the diagnosis of amyotrophic lateral sclerosis. *Amyotroph Lateral Scler Other Motor Neuron Disord.* 1 (5):293–299 (PubMed PMID: 11464847). Epub 2001/07/24. eng).
- da Rocha, A.J., Oliveira, A.S., Fonseca, R.B., Maia Jr., A.C., Buainain, R.P., Lederman, H.M., 2004 Oct. Detection of corticospinal tract compromise in amyotrophic lateral sclerosis with brain MR imaging: relevance of the T1-weighted spin-echo magnetization transfer contrast sequence. *AJNR Am. J. Neuroradiol.* 25 (9):1509–1515 (PubMed PMID: 15502129). Epub 2004/10/27. eng).
- Ellis, C.M., Simmons, A., Jones, D.K., Bland, J., Dawson, J.M., Horsfield, M.A., et al., 1999 Sep 22. Diffusion tensor MRI assesses corticospinal tract damage in ALS. *Neurology* 53 (5):1051–1058 (PubMed PMID: 10496265). Epub 1999/09/25. eng).
- Graham, J.M., Papadakis, N., Evans, J., Widjaja, E., Romanowski, C.A., Paley, M.N., et al., 2004 Dec 14. Diffusion tensor imaging for the assessment of upper motor neuron integrity in ALS. *Neurology* 63 (11):2111–2119 (PubMed PMID: 15596758). Epub 2004/12/15. eng).
- Gubbay, S.S., Kahana, E., Zilber, N., Cooper, G., Pintov, S., Leibowitz, Y., 1985. Amyotrophic lateral sclerosis. A study of its presentation and prognosis. *J. Neurol.* 232 (5):295–300 (PubMed PMID: 4056836). Epub 1985/01/01. eng).
- Jacob, S., Finsterbusch, J., Weishaupt, J.H., Khorram-Sefat, D., Frahm, J., Ehrenreich, H., 2003 Sep. Diffusion tensor imaging for long-term follow-up of corticospinal tract degeneration in amyotrophic lateral sclerosis. *Neuroradiology* 45 (9):598–600 (PubMed PMID: 12904924). Epub 2003/08/09. eng).
- Jenkinson, M., 2003 Jan. Fast, automated, N-dimensional phase-unwrapping algorithm. *Magn. Reson. Med.* 49 (1):193–197 (PubMed PMID: 12509838). Epub 2003/01/02. eng).
- Jenkinson, M., 2004. Improving the Registration of B0-distorted EPI Images Using Calculated Cost Function Weights. *Tenth IntConf on Functional Mapping of the Human Brain*.
- Jiang, H., van Zijl, P.C., Kim, J., Pearlson, G.D., Mori, S., 2006 Feb. DtiStudio: resource program for diffusion tensor computation and fiber bundle tracking. *Comput. Methods Prog. Biomed.* 81 (2):106–116 (PubMed PMID: 16413083). Epub 2006/01/18. eng).
- Kaufmann, P., Pullman, S.L., Shungu, D.C., Chan, S., Hays, A.P., Del Bene, M.L., et al., 2004 May 25. Objective tests for upper motor neuron involvement in amyotrophic lateral sclerosis (ALS). *Neurology* 62 (10):1753–1757 (PubMed PMID: 15159473). Epub 2004/05/26. eng).
- Leemans, A., Jones, D.K., 2009 Jun. The B-matrix must be rotated when correcting for subject motion in DTI data. *Magn. Reson. Med.* 61 (6):1336–1349 (PubMed PMID: 19319973). Epub 2009/03/26. eng).
- Matte, G.P., Pioro, E.P., 2010. Clinical features and natural history in ALS patients with upper motor neuron abnormalities on conventional brain MRI. *Neurology* 74 (Suppl. 2), A216.
- Medina, D.A., Gaviria, M., 2008 Aug. Diffusion tensor imaging investigations in Alzheimer's disease: the resurgence of white matter compromise in the cortical dysfunction of the aging brain. *Neuropsychiatr. Dis. Treat.* 4 (4):737–742 (PubMed PMID: 19043518). Pubmed Central PMCID: 2536541. Epub 2008/12/02. eng).
- Mitusmoto, H., Chad, D.A., Pioro, E.P., 1998. *Amyotrophic Lateral Sclerosis Contemporary Neurology Series*. Oxford University Press, Philadelphia.
- Ngai, S., Tang, Y.M., Du, L., Stuckey, S., 2007 Feb. Hyperintensity of the precentral gyral subcortical white matter and hypointensity of the precentral gyrus on fluid-attenuated inversion recovery: variation with age and implications for the diagnosis of amyotrophic lateral sclerosis. *AJNR Am. J. Neuroradiol.* 28 (2):250–254 (PubMed PMID: 17296988). Epub 2007/02/14. eng).
- Rajagopalan, V., Yue, G.H., Pioro, E.P., 2013 Oct. Brain white matter diffusion tensor metrics from clinical 1.5T MRI distinguish between ALS phenotypes. *J. Neurol.* 260 (10):2532–2540 (PubMed PMID: 23864396).
- Sach, M., Winkler, G., Glauche, V., Liepert, J., Heimbach, B., Koch, M.A., et al., 2004 Feb. Diffusion tensor MRI of early upper motor neuron involvement in amyotrophic lateral sclerosis. *Brain* 127 (Pt 2):340–350 (PubMed PMID: 14607785). Epub 2003/11/11. eng).
- Sage, C.A., Van Hecke, W., Peeters, R., Sijbers, J., Robberecht, W., Parizel, P., et al., 2009 Nov. Quantitative diffusion tensor imaging in amyotrophic lateral sclerosis: revisited. *Hum. Brain Mapp.* 30 (11):3657–3675 (PubMed PMID: 19404990). Epub 2009/05/01. eng).
- Schimrigk, S.K., Bellenberg, B., Schluter, M., Stieltjes, B., Drescher, R., Rexilius, J., et al., 2007 Apr. Diffusion tensor imaging-based fractional anisotropy quantification in the corticospinal tract of patients with amyotrophic lateral sclerosis using a probabilistic mixture model. *AJNR Am. J. Neuroradiol.* 28 (4):724–730 (PubMed PMID: 17416829). Epub 2007/04/10. eng).
- Smith, S.M., Jenkinson, M., Woolrich, M.W., Beckmann, C.F., Behrens, T.E., Johansen-Berg, H., et al., 2004. Advances in functional and structural MR image analysis and implementation as FSL. *NeuroImage* 23 (Suppl. 1):S208–S219 (PubMed PMID: 15501092). Epub 2004/10/27. eng).
- Wakana, S., Jiang, H., Nagae-Poetscher, L.M., van Zijl, P.C., Mori, S., 2004 Jan. Fiber tract-based atlas of human white matter anatomy. *Radiology* 230 (1):77–87 (PubMed PMID: 14645885).
- Wakana, S., Caprihan, A., Panzenboeck, M.M., Fallon, J.H., Perry, M., Gollub, R.L., et al., 2007 Jul 1. Reproducibility of quantitative tractography methods applied to cerebral white matter. *NeuroImage* 36 (3):630–644 (PubMed PMID: 17481925). Epub 2007/05/08. eng).
- Yagishita, A., Nakano, I., Oda, M., Hirano, A., 1994 May. Location of the corticospinal tract in the internal capsule at MR imaging. *Radiology* 191 (2):455–460 (PubMed PMID: 8153321). Epub 1994/05/01. eng).